Is it possible to enhance Raman scattering of single-walled carbon nanotubes by metal particles during chemical vapor deposition?

Ming Liu,[1] Rong Xiang,[1,2]* Wu Cao,[1] Haiqiang Zeng,[1] Yuquan Su,[1] Xuchun Gui,[1] Tianzhun Wu,[3] Shigeo Maruyama,[2] Zikang Tang[1,4]*

[1] State Key Laboratory of Optoelectronic Materials and Technologies, School of Physics and Engineering, Sun Yat-Sen University, Guangzhou 510275, China

[2] Department of Mechanical Engineering, The University of Tokyo, 7-3-1 Hongo, Bunkyo-ku, Tokyo 113-8656, Japan

[3] Institute of Biomedical and Health Engineering, Shenzhen Institutes of Advanced Technology, Chinese Academy of Sciences, Shenzhen 518055, China

[4] Department of Physics, Hong Kong University of Science and Technology, Clear Water Bay, Hong Kong, China

*Corresponding authors.
Tel.: +86-20-39943409 Fax: +86-20-39943262, E-mail address: xiangr2@mail.sysu.edu.cn (R. Xiang).
Tel.: Fax: E-mail address: phzktang@ust.hk (Z.K. Tang).

Abstract

We explore the possibility of using metal nano-particles to enhance the Raman scattering of single walled carbon nanotubes (SWCNTs) at high temperatures, with the aim of obtaining enhanced *in situ* Raman spectra of SWCNT during chemical vapor deposition (CVD). Particle position, metal type, film thickness, excitation wavelength are systematically optimized to meet the requirements for high temperature and *in situ* measurements. Au particles provide a weak but stable enhancement up to 1000°C, while the enhancement factors of Ag particles decrease at elevated temperatures due to morphology change and metal evaporation. After the morphology relating effects are eliminated, surface enhanced Raman scattering (SERS) of SWCNT is confirmed to be almost temperature independent in our SWCNT-Ag/Au system. Finally, *in situ* enhanced spectra with identifiable RBM peaks are obtained in a realistic CVD growth of SWCNTs. The mechanism behind the relatively low enhancement factor is also discussed.

1. Introduction

Single walled carbon nanotubes (SWCNTs) have attracted much attention in the past decades, due to their many outstanding properties and potential applications [1,2]. In many applications (e.g. as the transparent conductive layer in a solar cell [3] or as the channels in a field effect transistor[4]) SWCNTs with highly uniform properties are required. However, present growth techniques normally produce SWCNTs with mixed length, diameter, and conductivity. In this context, extensive and sustained efforts were made by both theorists and experimentalists to understand the growth mechanism of SWCNTs and to search for better solutions to control the key structural parameters [5-7].

Since the early stage of chemical vapor deposition (CVD) growth, researchers have attempted to monitor the growth process of SWCNTs in real time, because an *in situ* measurement always provides more direct and comprehensive information which can help to get a better understand of the nucleation, termination or growth selectivity. For example, ten years ago *in situ* TEM clearly revealed the reshaping of the catalyst particles and restructuring of mono-atomic step edges at atomic level [8]. Later, methods including real time reflectance [9,10], absorbance measurements [11,12], and optical imaging [13-15] have been proposed to monitor the growth process of vertically aligned carbon nanotubes (CNTs), which significantly accelerated the investigation and identification of CNTs' various growth and termination behaviors. More recently, Hofmann *et al.* performed a systematic *in situ* XPS measurement on the surface bounding during CVD of SWCNTs, and obtained a series of new understandings on catalyst-substrate interaction and catalyst phase transition [16,17]. Hart *et al.* introduced a high speed small angle X-ray scattering technique, which un-ambiguously revealed the quick evolution of catalyst from a film to particles during reduction and also the later size change during growth [18]. Chen *et al.* studied SWCNT growth and oxidation in an *in situ* thermogravimetric reactor and identified the role of working metal catalysts [19].

Raman spectroscopy is one of the most powerful techniques for SWCNT detection and structure confirmation [20,21]. In principle, *in situ* Raman scattering can provide

insights into both formation dynamics (quantity vs. time) and population evolution (distribution vs. time) of the obtained SWCNTs. For example, intensity and shape evolution of G band may suggest the overall growth deceleration during a CVD, as well as the proportion change between semiconducting and metallic SWCNTs. The evolution of each radial breathing mode (RBM) may even quickly reveal chirality dependent nucleation and termination behaviors. More importantly, for an *in situ* measurement, spectra can be continuously taken in the same CVD run at short intervals (e.g. 5 s). Obtaining the similar information using an *ex situ* Raman scattering will take enormously more experiments. However, within the limited progresses on *in situ* Raman scattering since the very pioneer work by Chiashi *et al.* [22], Raman intensity obtained at a high temperature during growth is almost always too weak to explicit the structure-relating fingerprints, e.g. position and shape of G-peak or [23-27] even RBM peaks [28,29]. Therefore, one interesting question that arises is whether it is scientifically and technically possible to enhance Rama scattering of SWCNTs during CVD growth by conventional enhancing techniques, e.g. metal nano-particles which are often recognized as surface enhance Raman scattering.

In this study, we are devoted to explore the possibility of enhancing Raman scattering of SWCNTs at CVD growth conditions using SERS metal nano-particles. One major difference from conventional SERS of SWCNTs [30,31] is that SERS measurements during a CVD (called "*in situ* SERS" hereafter) involves a high growth temperature (usually above 800°C), which brings new technical and scientific challenges. At the same time, previous SERS studied were seldom performed at temperatures above 300°C. Whether or not SERS effect still existing at a growth temperature has not yet been experimentally confirmed. Therefore, exploring SERS effect at CVD conditions become meaningful for both studying SWCNT growth and SERS study itself. In this context, we perform a systematic study on the metal position, metal type, particle size, excitation wavelength to seek the feasibility and, if feasible, the optimized configuration of *in situ* SERS. Finally, a weak but clear enhancement of Raman scattering during a realistic CVD is demonstrated by Ag

SERS. Though the enhancement factor is low at this stage, this work proves the concept of using SERS at high temperatures to enhance the Raman scattering during SWCNT CVD formation.

2. Experimental

2.1. Preparation of metal particles

Au, Ag, Cu, Pt particles are prepared on Si/SiO_2 (500 nm oxide layer) substrates by e-beam evaporation and post-annealing. The thickness of metal film is controlled by the deposition rate and time, and the particle size can be adjusted by the annealing temperature. The annealing time is 30 min in all cases unless described otherwise.

2.2. Transfer of SWCNT films

Transfer of SWCNT films is achieved by the following steps: 1) submerge the as-grown SWCNT sample (*i.e.* SWCNTs on Si/SiO_2 substrate) into a HF solution, which removes the SiO_2 layer and therefore detaches the SWCNT film from the Si substrate; 2) dilute the HF solution (with SWCNT film floating on top); 3) collect the floating SWCNT film by a SERS substrate (with metal particles) prepared in section 2.1.

2.3. Catalyst preparation and CVD growth

Catalyst for SWCNT growth is prepared by dip-coating [32]. Briefly, the substrate is submerged into a catalyst precursor solution (cobalt and molybdenum acetate in ethanol) and lifted at a speed of 4 cm/min. After coating, the substrate is annealed at 400°C for 5 min to decompose the acetates. SWCNTs are synthesized by alcohol catalytic CVD (ACCVD) using ethanol as the carbon source [33]. The CVD temperature is 800°C and the ethanol pressure is kept at 1.3 kPa. More details of the dip-coating and SWCNT growth can be found in our previous reports [11,34,35].

2.4. Characterization and Raman measurement

The obtained materials are characterized by an SEM (Hitachi S-4800, operated at 3 kV), and a Raman spectrometer (Horiba HR-800). High temperature and real time Raman spectra are measured in a Linkam CCR1000 reaction cell (accompanied with gas inlets and outlets for keeping a protective Ar atmosphere, a schematic of the

reaction cell is shown in Figure S1), which is put on the XYZ-motorized stage of the Raman system. Samples can be heated from room temperature up to 1000 °C in the reaction cell. The heating and cooling rate is 100°C /min in all measurements. Ethanol is brought into the reaction cell by bubbling a 15 sccm H_2 through an ethanol container. The Raman signal is collected by a long working distance lens, with the excitation wavelength of 488, 514, 633, and 785 nm.

3. Results and discussion

Different from room temperature SERS which has been extensively studied, high temperature SERS is a field that received much less attention previously [36-38]. This may be partly attributed to the few expecting applications of higher temperature SERS. Meanwhile, those organic molecules often used in SERS experiments are also not high temperature resistible, which may have limited even fundamental research on high temperature SERS. In real time monitoring CVD growth of SWCNT, however, SERS technique may provide a path to increase the weak Raman signal and to reveal more details of a formation process. High thermal stability also makes SWCNT a promising system for high temperature SERS studies. Therefore, a systematic exploration becomes both meaningful and possible in this context.

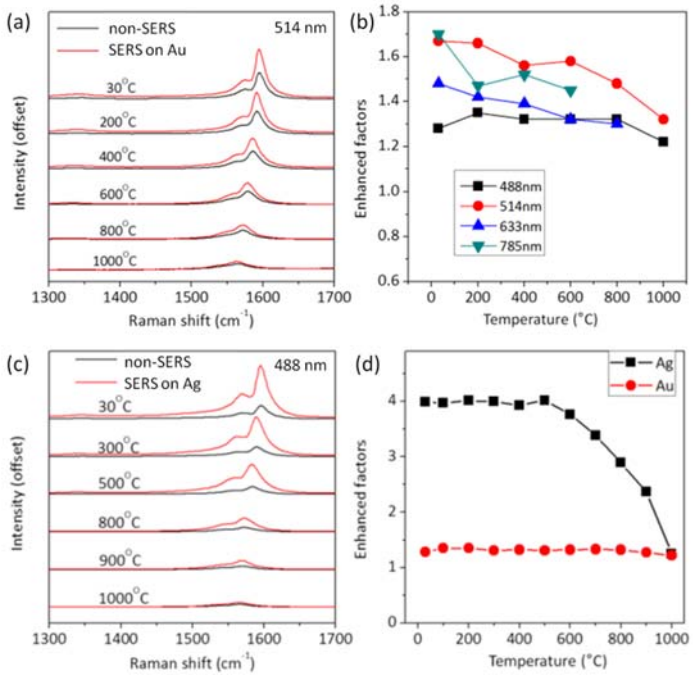

Figure 1. (a) Non-SERS spectra of SWCNT on SiO_2 substrate and SERS spectra of the same SWCNT film on Au deposited substrate at different temperatures (excitation laser 514 nm); (b) enhancement factor vs. temperature at different excitation wavelengths; (c) non-SERS spectra of SWCNT on SiO_2 substrate and SERS spectra of the same SWCNT film on Ag deposited substrate at different temperatures (excitation laser 488 nm); (d) a comparison of enhancement factor vs. temperature between Au and Ag at 488 nm excitation.

Figure 1a shows comparisons of SERS (red) and non-SERS (black) spectra of SWCNTs taken from 30 °C up to 1000 °C. A protective Ar atmosphere is introduced in the cell during the entire measurement to prevent oxidation of SWCNTs. Au, one of the most commonly used SERS metal, is pre-deposited onto a Si/SiO_2 substrate before the transfer of SWCNTs (metal-SWCNT structure in Figure S2). The SERS and non-SERS spectra are obtained in a small area to ensure precise identification of the enhancement (Figure S3a). In Figure 1a, high temperature brings at least two main changes to the Raman spectra. First, all peaks down shift to lower wavenumbers. This trend has been well recognized in previous studies and can be explained by the structure expansion and C-C bond softening [24,39,40]. Second, Raman intensity decreases significantly at evaluated temperatures (e.g., at 1000°C, only ~10% of original). However, if we compare G band intensity in SERS and non-SERS conditions, clear enhancements can be still observed at all temperatures. For example, the enhancement factor (defined as $I_{SERS}/I_{non\text{-}SERS}$) is 1.65 at room temperature and 1.5 at 800°C. Though an enhancement factor of less than two in this first study is un-expectedly small (reasons to explain later), there are about two wavenumber shift in G band to lower wavenumber (from 1592 to 1590 cm^{-1}) when metal particles are existing, which is one typical feature of SERS effect.

High temperature SERS effect is further confirmed at different excitation wavelengths (488, 514, 633, 785 nm). The enhancement factor vs. temperature is plotted in Figure 1b. There are slight drops with temperature but generally enhancements are observable at all excitations. In this experiment, strong red (from 800 °C) and IR (from 600 °C) background prohibited us from obtaining moderate spectra at 633 and 785 nm excitations. Therefore, red and IR lasers may not be

directly used as excitation when monitoring realistic growth processes, the temperature of which is mostly above 800 °C. For green (514 nm) and blue (488 nm) excitations, moderated spectra are obtained up to 1000 °C.

Leung *et al.* have previously calculated the influence of temperature on SERS effect [36]. In their theory, SERS effect decrease at elevated temperatures if the excitation wavelength is close or higher than the resonant peak of the metal particle. However, if the excitation wavelength is much shorter, SERS effect is generally insensitive to temperature. In Figure 1b, we notice the slopes of 785 nm and 633 nm (longer wavelength) seem to be larger than those of 488 nm, which is in agreement with Leung's predictions. Although more systematic experiments may be needed to confirm the versatility, this preliminary work clearly suggest SERS effect can survive a high temperature both theoretically and experimentally.

Similar measurements are performed on Ag. For Ag SERS, a higher enhancement factor up to four is achieved, as shown in Figure 1c. Further study on wavelength dependence also revealed 488 nm (no influence of background irradiation) excitation has the largest enhancement effect among all our available lasers. Therefore, the combination of Ag with 488 nm excitation becomes presently most promising configuration for an *in situ* SERS study in terms of getting a large (relatively) enhancement factor and a clean background. However, as shown in Figure 1d, though Ag has generally larger enhancement factors than Au at all temperatures, a drastic decrease is observed from 600°C. Considering that the Ag particles in this experiment are annealed at 650°C before use (to let metal film aggregate into particles), we speculate this decrease originated from the poor stability of Ag at high temperatures. Similar experiments are also repeated on Cu, and Pt particles. We include Pt since its higher melting temperature may possibly benefit the thermal stability in an *in situ* measurement (e.g. at 800 °C). However, unfortunately both Pt and Cu show almost no enhancement at all our excitations (e.g. see Figure S3b), possibly due to their relatively smaller Raman cross-sections and shorter resonant wavelength (near UV) [41].

In order to explain the enhancement decrease at high temperatures for Ag SERS, we propose an experiment to investigate the influence of annealing temperature on morphology of Ag, and its corresponding Raman enhancement. First, a SWCNT film is transferred on to a substrate with 50 nm as evaporated Ag film. The SERS and non-SERS spectra are measured at room temperature. A SEM image is also taken at same point where Raman spectra are obtained. After Raman and SEM characterizations, the substrate is heated to 200°C, kept for 10 min, and then cooled to room temperature. This heating and cooling process are repeated at 400, 600, 800°C. For each cycle, SEM images are taken after cooling, and Raman spectra are measured at both high temperatures and room temperature. The experimental profile and the obtained results are summarized in Figure 2.

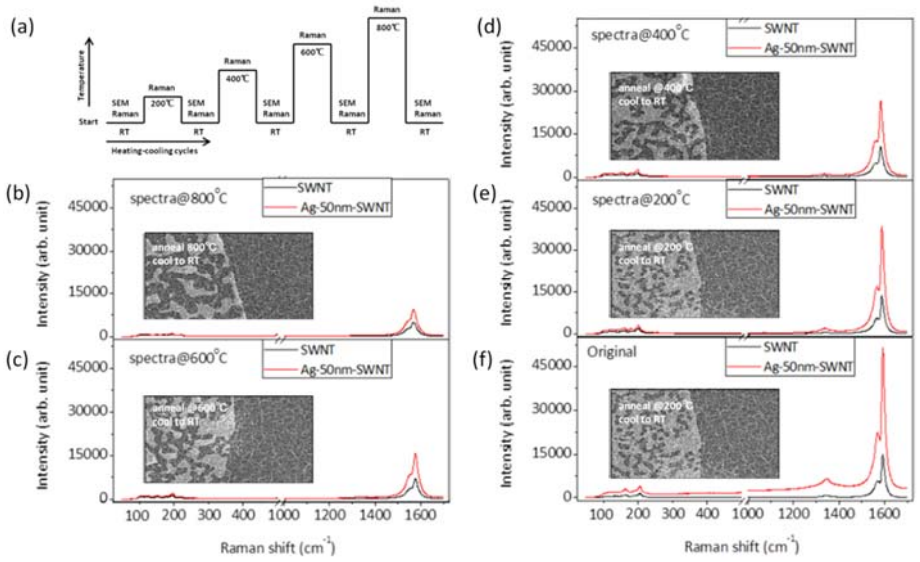

Figure 2. (a) An experimental scheme recording the morphology and enhancement factor change with annealing temperature; (b)-(f) Representative Raman spectra and corresponding SEM images (insets) of the "SWCNT on Ag" structure in each annealing cycle.

The representative SEM images (insets) after each cycle in Figure 2b-f clearly reveal that Ag evolves from a continuous film to separate islands. The enhancement factor gradually decreases from 3.2 (before annealing) to less than 2 (after 800°C annealing). However, at each morphology, if comparing the enhancement factors at

elevated temperature (before cooling) and room temperature (after cooling) in Figure 3, we find the "cold" and "hot" enhancement factors are almost identical (e.g. for the 600°C annealed substrate, 2.2 at 600°C and 2.3 back at room temperature). This comparison suggests that the decrease in Figure 1d originates from the temperature induced morphology change. The SERS effect itself is weakly dependent, or almost independent, on temperature at a fixed morphology. Besides the change from a film to islands, evaporation of Ag may be another reason for the enhancement decay, because density of the island/particles starts to decrease from 600 °C, and Ag completely disappears at 1000°C (not shown).

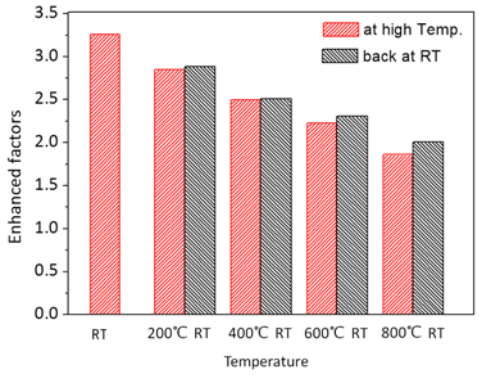

Figure 3. A comparison of enhancement factors at hot (high temperature, red) and cold (room temperature, black) conditions for a fixed morphology of Ag particles, suggesting the SERS effect in our system is weakly temperature dependent and the enhancement decay merely originates high temperature induced morphology change.

Though SERS effect is confirmed to be temperature insensitive in our system, the enhancement factor is much lower than expected, since SERS is often recognized to be able to enhance Raman signal by many orders of magnitude. We attribute this low enhancement factor to the following two reasons. First, Raman scattering of SWCNT is well known as a resonant process, for a single SWCNT, it is easy see a strong SERS effect if the tube is not in resonance to the excitation. For the entire SWCNT film, however, since there are always tubes that are resonant to the excitation, the signal obtained is already resonance enhanced. Therefore, SERS effect in resonant Raman is much less significant. The difference between resonance SERS and SERS spectra were carefully investigated before by M. Dresselhaus.[42] Second, since the

inter-particle distance is about tens of nm, possibly the SWCNTs are in plane not uniformly enhanced, and only at local areas were SWCNTs strongly SERS enhanced. Also, the SWCNT is normally tens of nm thick, the SWCNT may be also not uniformly enhanced in Z direction. Though at this stage we are not able to quantify the percentage of SWCNTs that are enhanced, very likely the enhancement factor can be further improved in future studies, e.g. by controlling SWCNT growth directions.

After the feasibility of high temperature SERS is confirmed, we present a preliminary demonstration of a during growth *in situ* enhancement. Figure 4 shows the *in situ* obtained Raman spectra in a realistic CVD growth at 900°C. In this experiment, 5 nm Ag (effect of initial deposition thickness is shown in Figure S4) is deposited onto Si/SiO_2 substrate and 488 nm laser is used as excitation. Co/Mo catalyst is coated onto the substrates by dip-coating. The catalyst preparation, CVD parameter and Raman measurement are kept strictly the same in (a) and (b). On bare Si/SiO_2 wafer (non-SERS condition), G band is about 100 after a 600 s growth. On the SERS active substrate, however, signal reaches about 600. Mostly importantly, a clear peak is observed in the RBM region of the *in situ* SERS spectra, whereas in the non-SERS situation, no identifiable RBM peaks are observed. The exposure time for each spectrum in this experiment is short (5s) and the laser power is also fairly weak (few mW). Improved spectra may be obtained if longer exposure and stronger laser are applied. Furthermore, the catalyst preparation and CVD condition may be also not optimized in the present reaction cell (much smaller than conventional lab-scale CVD furnaces). Therefore, though at this stage the obtained *in situ* spectra are still too noisy and can hardly reveal the growth dynamics of each single chirality SWCNT, there should still plenty of room to improve the experiment design and the spectrum quality in the future studies. Nonetheless, we believe the concept and potential application of this during CVD *in situ* SERS has been to this end well proven.

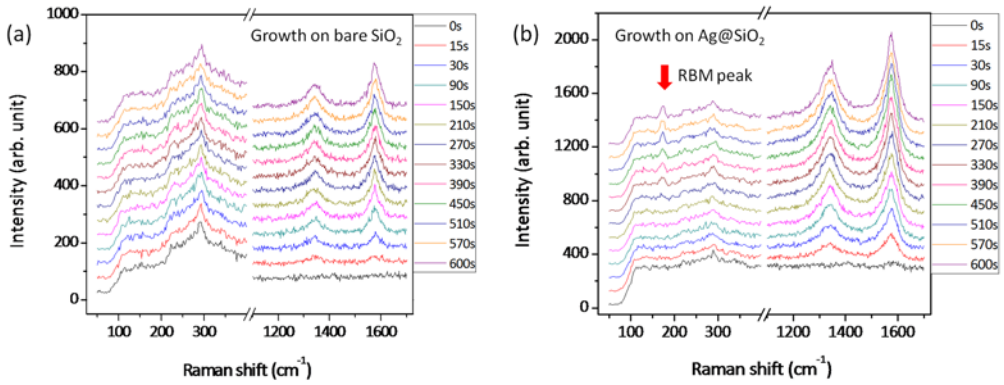

Figure 4. *In situ* Raman spectra taken at 900°C in a realistic CVD growth on (a) a bare Si/SiO_2 substrate and (b) a SERS active substrate, suggesting Raman scattering of SWCNTs is about six times enhanced during the growth by the as-deposited Ag particles.

Finally, one may be concerned with the possible influences of the SERS particles on SWCNT growth, particularly after recent advances having shown noble metals [43] like Pt, Au, Ag, and other transition metal like Cu [44] can also catalyze the nucleation of SWCNTs. Since the diameter of enhance media (e.g. Ag) so far used in the present study are all larger than 50 nm, which is way beyond the size range (usually < 5 nm) that can catalyze SWCNT formation, we tend to believe growth and enhancement are two rather independent processes with weak influence to each other. To ensure this point, we compare SEM images of SWCNT grown on two substrates and confirm that there are no noticeable difference in CNT yield with and without media coating. At the same time, we also observe a slight down shift of G-band for the SWCNTs grown on SERS media covered substrate, which convince us the increase of Raman signal is a SERS effect. One other concern is that G and RBM peaks of SWCNTs shift and broaden at high temperatures, which may bring additional challenges for spectrum interpretation (e.g. chirality assignment). However, this interpretation should always be possible as long as the correlation between a room and high temperature spectrum can be known (e.g., by an experimental or theoretical approach). Nonetheless, more efforts are absolutely needed before high quality *in situ*

Raman spectra and more structure relating information can be obtained from realistic CVDs.

4. Conclusions

To conclude, we explored the possibility of using SERS techniques at high temperatures, with the aim of enhancing Raman signal of SWCNTs at realistic CVD growth conditions. Particle position, metal type, particle size, and excitation wavelength were systematically sieved to meet the requirements of *in situ* measurements. Au was able to provide a small but stable enhancement factor up to 1000°C. Ag particles presented a relatively larger enhancement factor but the enhancement decayed quickly above 1000°C. However, the comparison between high temperatures enhancement factor and room temperature enhancement factor at a fixed morphology confirmed weak temperature dependence for SWCNT SERS. Finally, an *in situ* Raman spectra with identifiable RMB peaks were obtained using Ag SERS. We expect this work can provide the first step toward enhancing Raman scattering of SWCNT during realistic CVD growths. Future work may be focused on the improving the low enhancement factors as well as the poor stability of SERS particles at high temperatures.

Acknowledgments

Part of this work was financially supported by National Science Foundation of China (51002190), Guangdong Provincial Natural Science Foundation of China (2011040004714) and the open funds of State Key Laboratory of Optoelectronic Materials and Technologies.

References

[1] Baughman RH, Zakhidov AA, de Heer WA Carbon nanotubes - the route toward applications. *Science* 2002; *297*(5582): 787-92.

[2] De Volder MFL, Tawfick SH, Baughman RH, Hart AJ Carbon Nanotubes: Present and Future Commercial Applications. *Science* 2013; *339*(6119): 535-39.

[3] Rowell MW, Topinka MA, McGehee MD, Prall HJ, Dennler G, Sariciftci NS, et al. Organic solar cells with carbon nanotube network electrodes. *Appl Phys Lett* 2006; *88*(23).

[4] Ding L, Tselev A, Wang JY, Yuan DN, Chu HB, McNicholas TP, et al. Selective Growth of Well-Aligned Semiconducting Single-Walled Carbon Nanotubes. *Nano Lett* 2009; *9*(2): 800-05.

[5] Ding F, Bolton K, Rosen A Nucleation and growth of single-walled carbon nanotubes: A molecular dynamics study. *J Phys Chem B* 2004; *108*(45): 17369-77.

[6] Page AJ, Ohta Y, Irle S, Morokuma K Mechanisms of Single-Walled Carbon Nanotube Nucleation, Growth, and Healing Determined Using QM/MD Methods. *Accounts Chem Res* 2010; *43*(10): 1375-85.

[7] Tessonnier JP, Su DS Recent Progress on the Growth Mechanism of Carbon Nanotubes: A Review. *Chemsuschem* 2011; *4*(7): 824-47.

[8] Helveg S, Lopez-Cartes C, Sehested J, Hansen PL, Clausen BS, Rostrup-Nielsen JR, et al. Atomic-scale imaging of carbon nanofibre growth. *Nature* 2004; *427*(6973): 426-29.

[9] Geohegan DB, Puretzky AA, Ivanov IN, Jesse S, Eres G, Howe JY In situ growth rate measurements and length control during chemical vapor deposition of vertically aligned multiwall carbon nanotubes. *Appl Phys Lett* 2003; *83*(9): 1851-53.

[10] Puretzky AA, Geohegan DB, Jesse S, Ivanov IN, Eres G In situ measurements and modeling of carbon nanotube array growth kinetics during chemical vapor deposition. *Appl Phys a-Mater* 2005; *81*(2): 223-40.

[11] Maruyama S, Einarsson E, Murakami Y, Edamura T Growth process of vertically aligned single-walled carbon nanotubes. *Chem Phys Lett* 2005; *403*(4-6): 320-23.

[12] Einarsson E, Murakami Y, Kadowaki M, Maruyama S Growth dynamics of vertically aligned single-walled carbon nanotubes from in situ measurements. *Carbon* 2008; *46*(6): 923-30.

[13] Hasegawa K, Noda S Real-time monitoring of millimeter-tall vertically aligned single-walled carbon nanotube growth on combinatorial catalyst library. *Jpn J Appl Phys* 2010; *49*(8R): 085104.

[14] Yasuda S, Futaba DN, Yumura M, Iijima S, Hata K Diagnostics and growth control of single-walled carbon nanotube forests using a telecentric optical system for in situ height monitoring. *Appl Phys Lett* 2008; *93*(14): 143115.

[15] Zhang Q, Huang JQ, Zhao MQ, Qian WZ, Wei F Carbon Nanotube Mass Production: Principles and Processes. *Chemsuschem* 2011; *4*(7): 864-89.

[16] Hofmann S, Sharma R, Ducati C, Du G, Mattevi C, Cepek C, et al. In situ observations of catalyst dynamics during surface-bound carbon nanotube nucleation. *Nano Lett* 2007; *7*(3): 602-08.

[17] Mattevi C, Wirth CT, Hofmann S, Blume R, Cantoro M, Ducati C, et al. In-situ X-ray photoelectron spectroscopy study of catalyst-support interactions and growth of carbon nanotube forests. *J Phys Chem C* 2008; *112*(32): 12207-13.

[18] Meshot ER, Verploegen E, Bedewy M, Tawfick S, Woll AR, Green KS, et al. High-Speed in Situ X-ray Scattering of Carbon Nanotube Film Nucleation and Self-Organization. *Acs Nano* 2012; *6*(6): 5091-101.

[19] Chen T-C, Zhao M-Q, Zhang Q, Tian G-L, Huang J-Q, Wei F In Situ Monitoring the Role of Working Metal Catalyst Nanoparticles for Ultrahigh Purity Single-Walled Carbon Nanotubes. *Adv Funct Mater* 2013; *23*(40): 5066-73.

[20] Bandow S, Chen G, Sumanasekera GU, Gupta R, Yudasaka M, Iijima S, et al. Diameter-selective resonant Raman scattering in double-wall carbon nanotubes. *Phys Rev B* 2002; *66*(7).
[21] Dresselhaus MS, Dresselhaus G, Saito R, Jorio A Raman spectroscopy of carbon nanotubes. *Phys Rep* 2005; *409*(2): 47-99.
[22] Chiashi S, Murakami Y, Miyauchi Y, Maruyama S Cold wall CVD generation of single-walled carbon nanotubes and in situ Raman scattering measurements of the growth stage. *Chem Phys Lett* 2004; *386*(1-3): 89-94.
[23] Jorio A, Saito R, Hafner JH, Lieber CM, Hunter M, McClure T, et al. Structural (n,m) Determination of Isolated Single-Wall Carbon Nanotubes by Resonant Raman Scattering. *Phys Rev Lett* 2001; *86*(6): 1118-21.
[24] Jorio A, Fantini C, Dantas MSS, Pimenta MA, Souza AG, Samsonidze GG, et al. Linewidth of the Raman features of individual single-wall carbon nanotubes. *Phys Rev B* 2002; *66*(11).
[25] Li-Pook-Than A, Lefebvre J, Finnie P Phases of Carbon Nanotube Growth and Population Evolution from in Situ Raman Spectroscopy during Chemical Vapor Deposition. *J Phys Chem C* 2010; *114*(25): 11018-25.
[26] Jorio A, Pimenta M, Souza Filho A, Saito R, Dresselhaus G, Dresselhaus M Characterizing carbon nanotube samples with resonance Raman scattering. *New J Phys* 2003; *5*(1): 139.
[27] Maruyama B, Curtarolo S, Semiatin S, Hooper D, Sargent G, Rao R, et al. Revealing the Impact of Catalyst Phase Transition on Carbon Nanotube Growth by in Situ Raman Spectroscopy. *ACS Nano* 2013; *7*(2): 1100-07.
[28] Huong PV, Cavagnat R, Ajayan PM, Stephan O Temperature-dependent vibrational spectra of carbon nanotubes. *Phys Rev B* 1995; *51*(15): 10048-51.
[29] Picher M, Anglaret E, Arenal R, Jourdain V Self-Deactivation of Single-Walled Carbon Nanotube Growth Studied by in Situ Raman Measurements. *Nano Lett* 2009; *9*(2): 542-47.
[30] Lefrant S Raman and SERS studies of carbon nanotube systems. *Curr Appl Phys* 2002; *2*(6): 479-82.
[31] Kneipp K, Kneipp H, Corio P, Brown S, Shafer K, Motz J, et al. Surface-enhanced and normal Stokes and anti-Stokes Raman spectroscopy of single-walled carbon nanotubes. *Phys Rev Lett* 2000; *84*(15): 3470.
[32] Murakami Y, Miyauchi Y, Chiashi S, Maruyama S Direct synthesis of high-quality single-walled carbon nanotubes on silicon and quartz substrates. *Chem Phys Lett* 2003; *377*(1-2): 49-54.
[33] Maruyama S, Kojima R, Miyauchi Y, Chiashi S, Kohno M Low-temperature synthesis of high-purity single-walled carbon nanotubes from alcohol. *Chem Phys Lett* 2002; *360*(3-4): 229-34.
[34] Xiang R, Einarsson E, Murakami Y, Shiomi J, Chiashi S, Tang ZK, et al. Diameter Modulation of Vertically Aligned Single-Walled Carbon Nanotubes. *Acs Nano* 2012; *6*(8): 7472-79.
[35] Xiang R, Wu TZ, Einarsson E, Suzuki Y, Murakami Y, Shiomi J, et al. High-Precision Selective Deposition of Catalyst for Facile Localized Growth of Single-Walled Carbon Nanotubes. *J Am Chem Soc* 2009; *131*(30): 10344-+.
[36] Leung PT, Hider MH, Sanchez EJ Surface-enhanced Raman scattering at elevated temperatures. *Phys Rev B* 1996; *53*(19): 12659.
[37] Chen C, Chiang H-P, Leung P, Tsai D Temperature dependence of enhanced optical absorption and Raman spectroscopy from metallic nanoparticles. *Solid State Commun* 2008; *148*(9): 413-16.
[38] Yang XA, Wang DC, Zhu JJ, Gu C, Zhang JZ In-situ reversible temperature-dependent surface enhanced Raman scattering study using optical fibers. *Chem Phys Lett* 2010; *495*(1-3): 109-12.
[39] Zhang Y, Xie L, Zhang J, Wu Z, Liu Z Temperature coefficients of Raman frequency of individual

single-walled carbon nanotubes. *J Phys Chem C* 2007; *111*(38): 14031-34.
[40] Li H, Yue K, Lian Z, Zhan Y, Zhou L, Zhang S, et al. Temperature dependence of the Raman spectra of single-wall carbon nanotubes. *Appl Phys Lett* 2000; *76*(15): 2053-55.
[41] Garcia MA Surface plasmons in metallic nanoparticles: fundamentals and applications. *J Phys D Appl Phys* 2011; *44*(28).
[42] Corio P, Brown SDM, Marucci A, Pimenta MA, Kneipp K, Dresselhaus G, et al. Surface-enhanced resonant Raman spectroscopy of single-wall carbon nanotubes adsorbed on silver and gold surfaces. *Phys Rev B* 2000; *61*(19): 13202-11.
[43] Takagi D, Homma Y, Hibino H, Suzuki S, Kobayashi Y Single-walled carbon nanotube growth from highly activated metal nanoparticles. *Nano Lett* 2006; *6*(12): 2642-45.
[44] Zhou WW, Han ZY, Wang JY, Zhang Y, Jin Z, Sun X, et al. Copper catalyzing growth of single-walled carbon nanotubes on substrates. *Nano Lett* 2006; *6*(12): 2987-90.

Toward surface-enhanced Raman scattering during growth of single-walled carbon nanotube

Ming Liu,[1] Rong Xiang,[1,2]* Wu Cao,[1] Haiqiang Zeng,[1] Yuquan Su,[1] Xuchun Gui,[1] Tianzhun Wu,[3] Shigeo Maruyama,[2] Zikang Tang[1,4]*

[1] State Key Laboratory of Optoelectronic Materials and Technologies, School of Physics and Engineering, Sun Yat-Sen University, Guangzhou 510275, China

[2] Department of Mechanical Engineering, The University of Tokyo, 7-3-1 Hongo, Bunkyo-ku, Tokyo 113-8656, Japan

[3] Institute of Biomedical and Health Engineering, Shenzhen Institutes of Advanced Technology, Chinese Academy of Sciences, Shenzhen 518055, China

[4] Department of Physics, Hong Kong University of Science and Technology, Clear Water Bay, Hong Kong, China

*Corresponding authors.
Tel.: +86-20-39943409 Fax: +86-20-39943262, E-mail address: xiangr2@mail.sysu.edu.cn (R. Xiang).
Tel.: Fax: E-mail address: phzktang@ust.hk (Z.K. Tang).

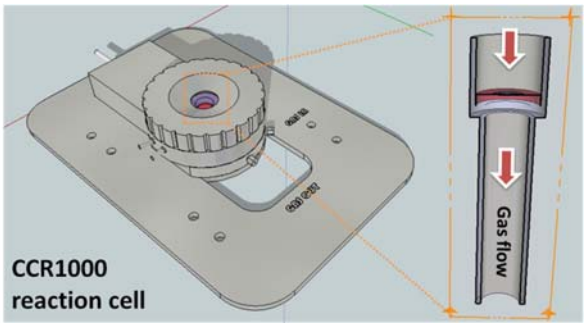

Figure S1: Schematic of the reaction cell (Linkam CCR1000) equipped on Raman spectrometer for high temperature and *in situ* Raman measurement. Arrows indicate the direction of gas (Ar in a protective atmosphere and Ar/H_2/Ethanol in a growth atmosphere) flow.

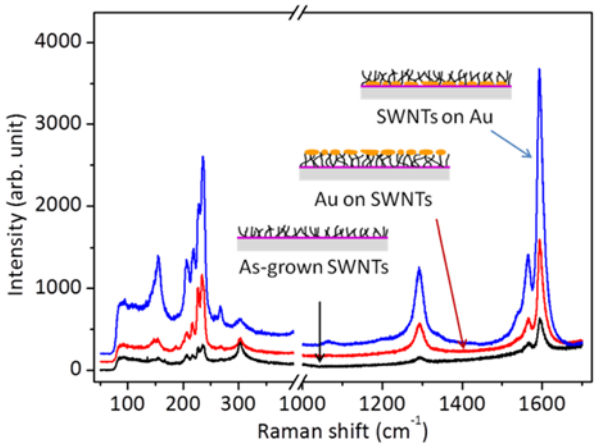

Figure S2: Characteristic Raman spectra obtained from an as-grown SWCNT film (non-SERS condition), the same SWCNT film with Au particles deposited on top, and the same SWCNT film transferred onto a Au particle coated substrate. The wavelength of the excitation laser is 785 nm.

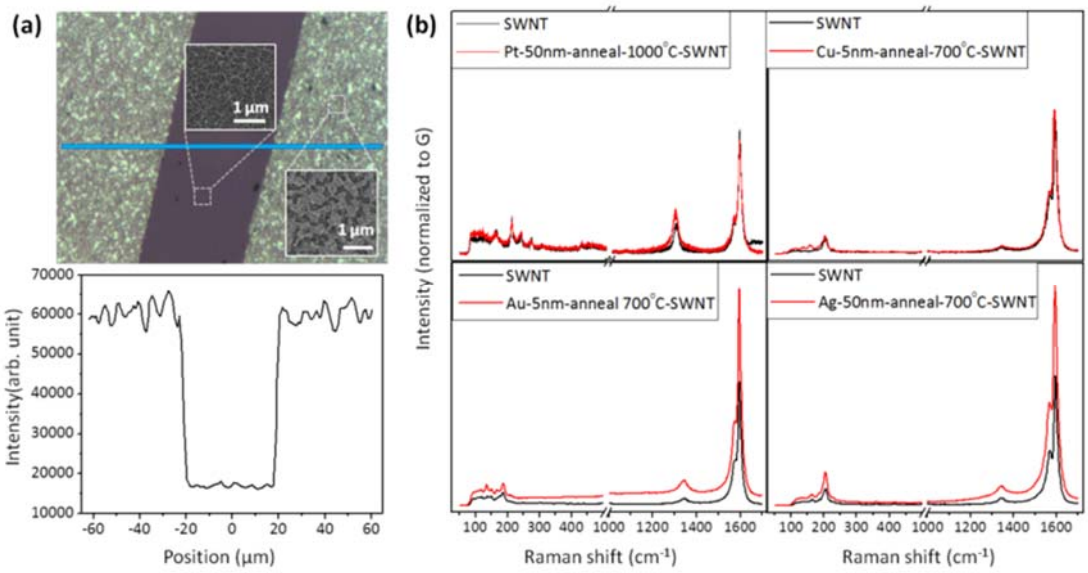

Figure S3: (a) Microscopic images (optical image with SEM micrographs as insets) and G band line scan of SWCNT films transferred onto a Si substrate partly covered with metal particles; (b) characteristic Raman spectra of SWCNTs at the areas without (non-SERS, black line) and with metal particles (SERS, red line). The effects of Pt, Cu, Au, Ag are investigated.

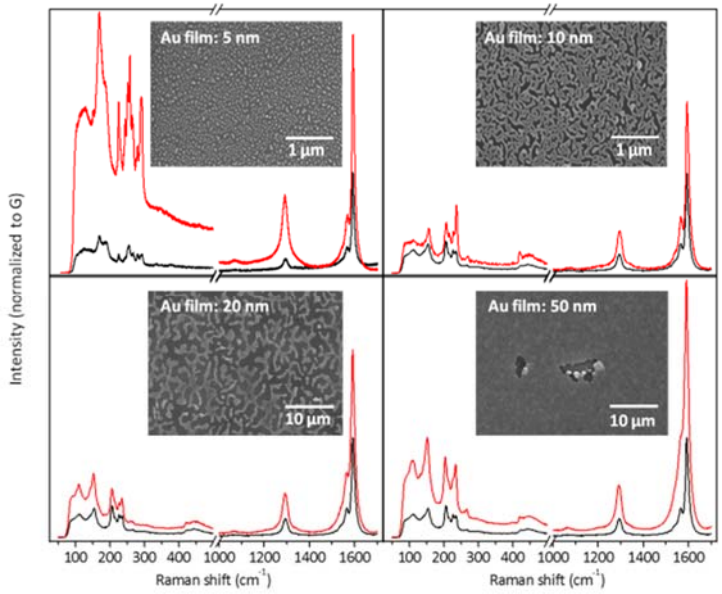

Figure S4. Characteristic non-SERS (black) and SERS (red) spectra of SWCNTs on Au film with different initial deposition thickness (5, 10, 20 and 50 nm), with SEM images of the metal particles shown as insets. If enhancement factors are similar, thinner metal film is preferred for *in situ* SERS since there is larger space for catalyst deposition and therefore SWCNT growth.